

SUPPORTING INFORMATION

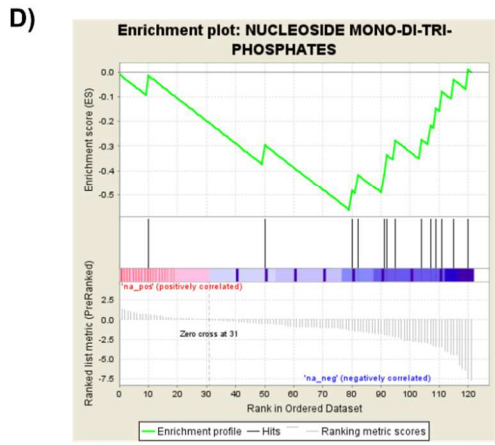
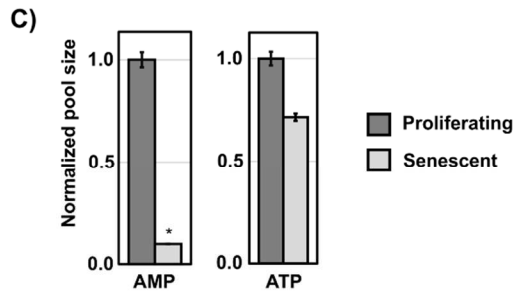
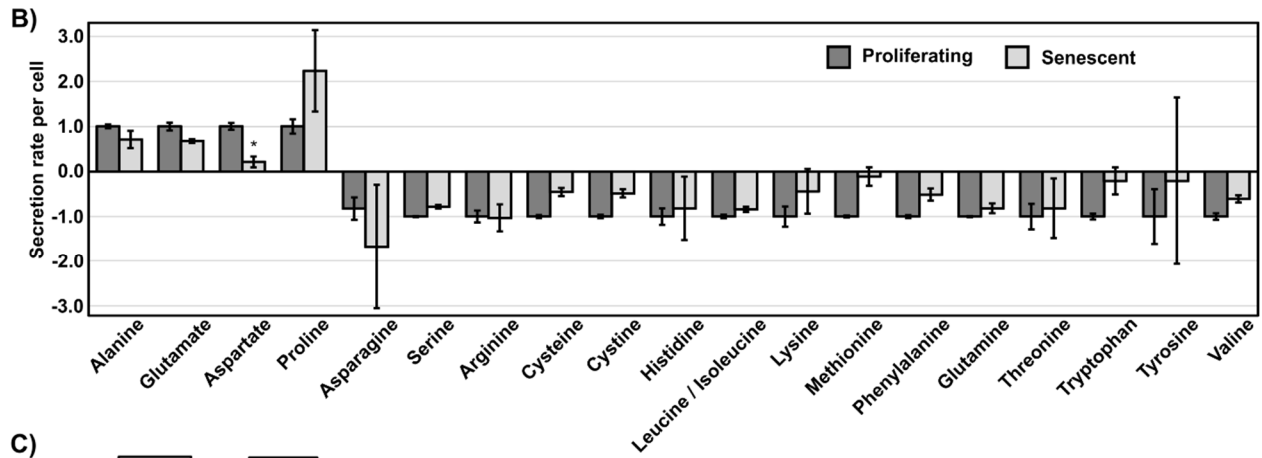
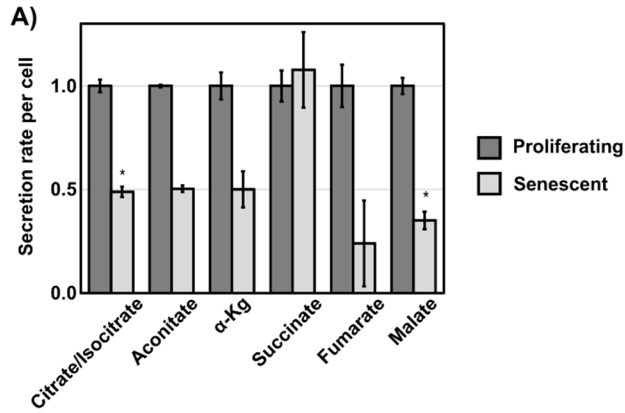
Inhibition of nucleotide synthesis mediates replicative senescence of human mammary epithelial cells

Alireza Delfarah¹, Sydney Parrish¹, Jesse Yang¹, Frances Seo¹, Si Li¹, Pin Wang¹, and Nicholas A. Graham^{1,2}

From the ¹Mork Family Department of Chemical Engineering and Materials Science; ²Norris Comprehensive Cancer Center, University of Southern California, Los Angeles, 90089

Running title: *Nucleotide synthesis regulates epithelial cell senescence*

To whom correspondence should be addressed: Corresponding author: Nicholas A. Graham, University of Southern California, Los Angeles, 3710 McClintock Ave., RTH 509, Los Angeles, CA 90089. Phone: 213-240-0449; E-mail: nagraham@usc.edu



Replicative senescence pool sizes				
COMPOUND CLASS	SIZE	NES	NOM p-val	FDR q-val
AMINO ACIDS	16	1.89	0.01	0.05
HYDROPHOBIC AMINO ACIDS	5	1.87	0.01	0.03
POLAR AMINO ACIDS	8	1.49	0.07	0.15
NUCLEOBASES	6	1.36	0.14	0.20
NUCLEOSIDES	5	1.04	0.40	0.48
URACIL DERIVATIVES	5	1.03	0.40	0.41
PENTOSE PHOSPHATE PATHWAY	6	-0.69	0.85	0.86
GUANINE DERIVATIVES	5	-0.75	0.77	0.86
GLYCOLYSIS	6	-0.84	0.65	0.82
HYPOXANTHINE DERIVATIVES	8	-0.94	0.51	0.75
THYMINE DERIVATIVES	5	-1.05	0.37	0.64
DEOXYNUCLEOSIDE MONO-DI-TRI-PHOSPHATE	10	-1.52	0.06	0.13
CYTOSINE DERIVATIVES	9	-1.55	0.06	0.15
TCA CYCLE	7	-1.72	0.02	0.08
NUCLEOSIDE MONOPHOSPHATES	5	-1.88	0.01	0.05
NUCLEOSIDE MONO-DI-TRI-PHOSPHATES	13	-2.35	0.0004	0.003

Higher concentration in senescent HMEC

Higher concentration in proliferating HMEC

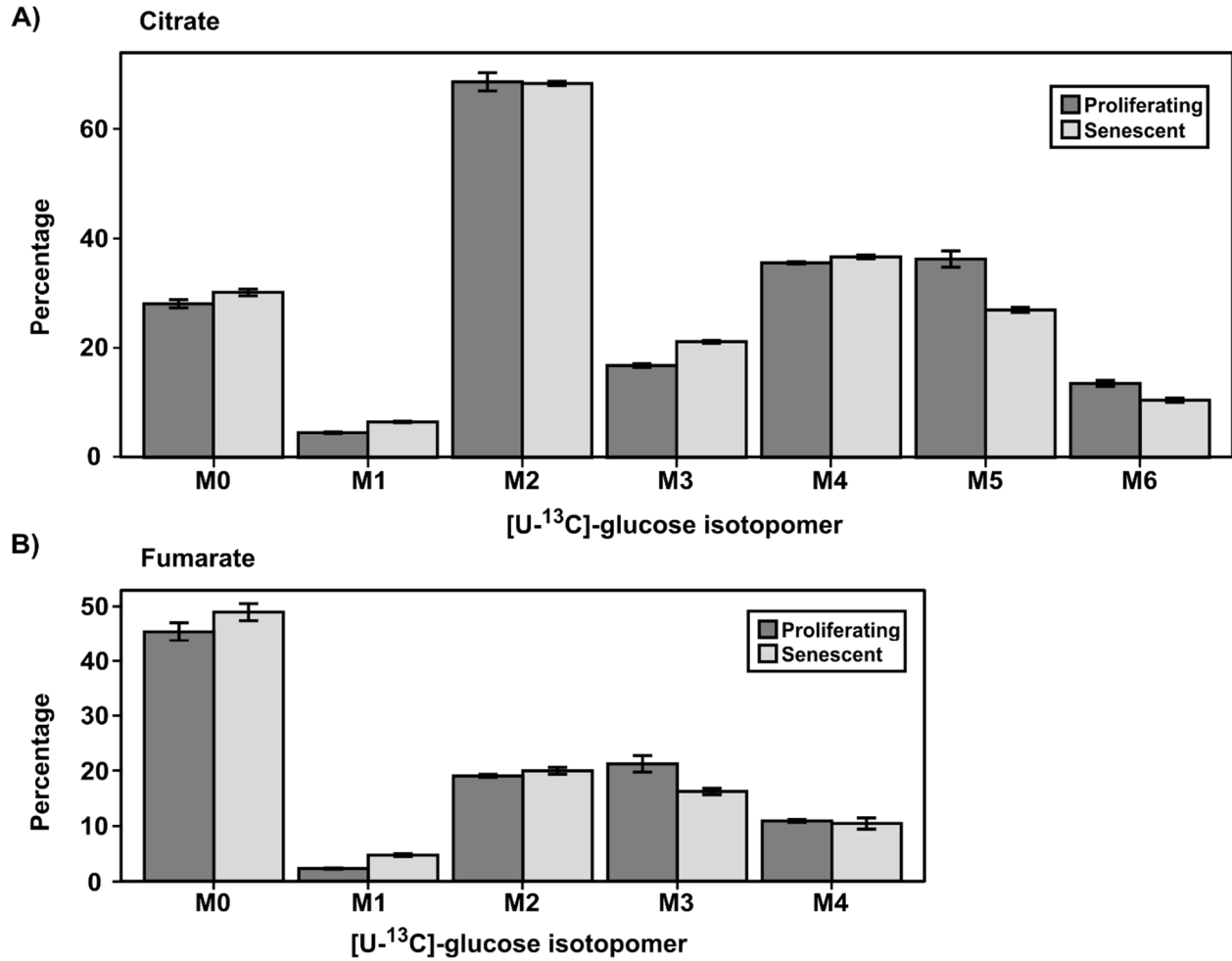
Supporting Fig. S1: Extracellular medium analysis of amino acid and TCA cycle metabolites, intracellular AMP/ATP levels, and MSEA analysis of senescent HMEC intracellular metabolite pools

A) Extracellular metabolite secretion data for TCA cycle metabolites in proliferating and senescent HMEC. Metabolite extracts from blank and conditioned media were analyzed by LC-MS. Secretion or uptake values were normalized to integrated cell number. Secreted metabolites have positive values, and consumed metabolites have negative values. * denotes p-value less than 0.05 by FDR-corrected Student's t-test. See Supporting Table S1 for all measured metabolites.

B) Same as in A for amino acids. * denotes p-value less than 0.05 by FDR-corrected Student's t-test. See Supporting Table S1 for all measured metabolites.

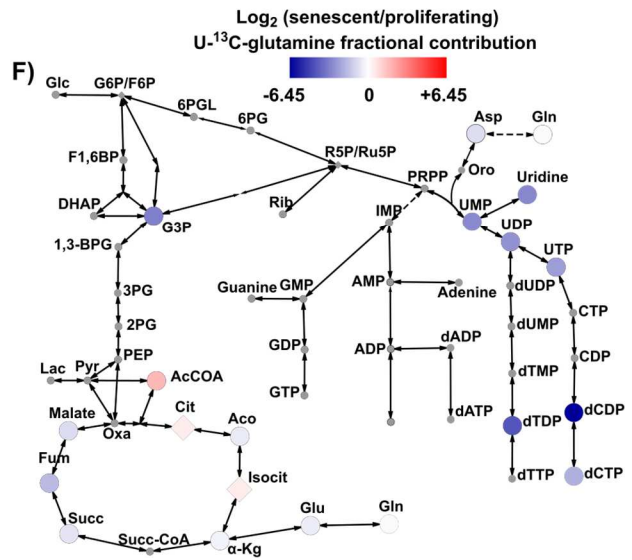
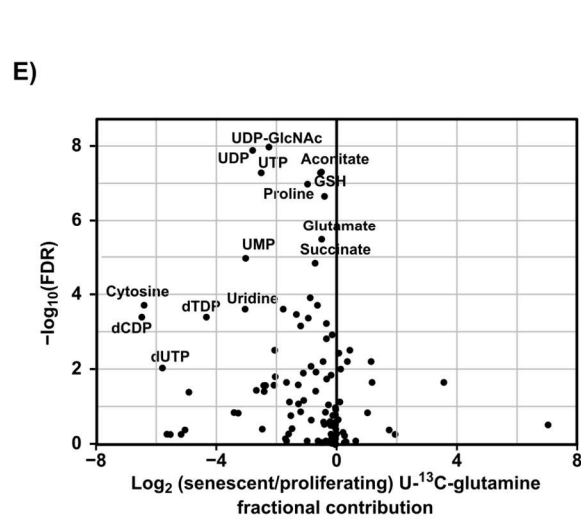
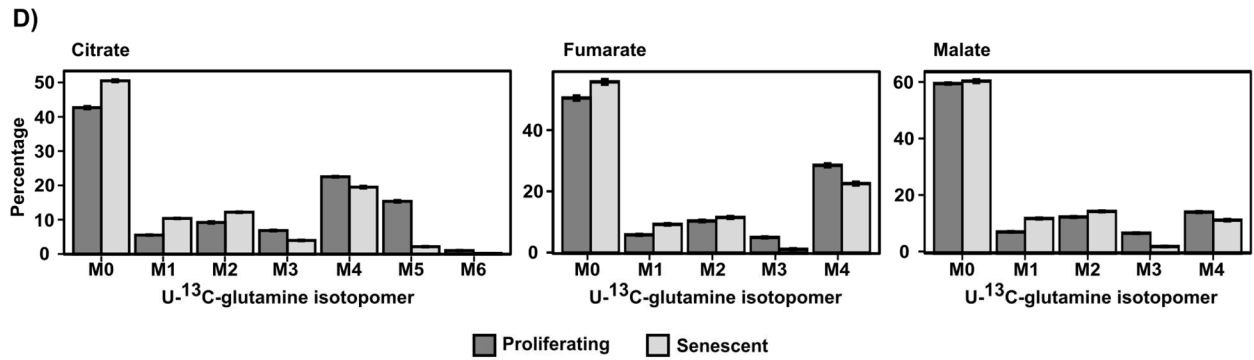
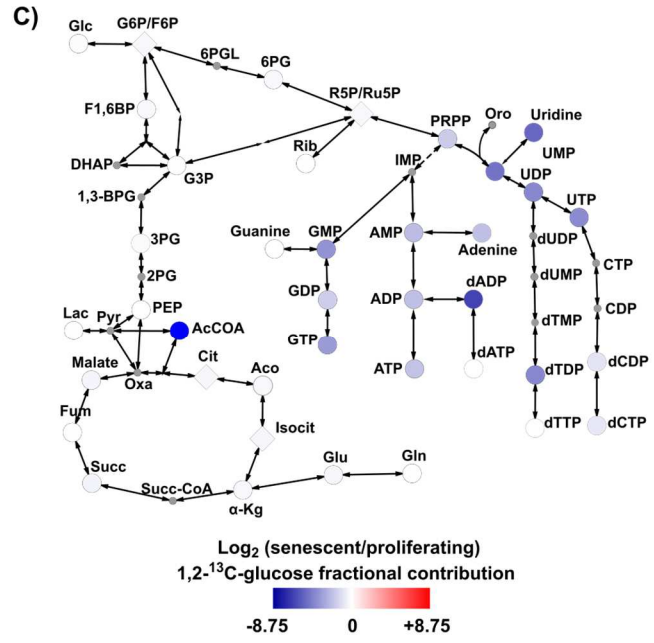
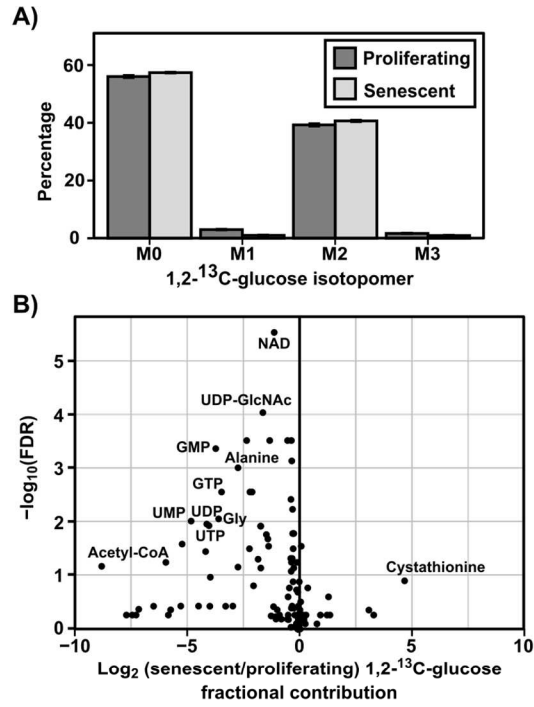
C) Intracellular pool sizes of AMP and ATP of proliferating and senescent HMEC. * denotes p-value less than 0.05 by FDR-corrected Student's t-test. See Supporting Table S2 for all measured metabolites.

D) Metabolite set enrichment analysis (MSEA) analysis for intracellular metabolites pool sizes of proliferating and senescent HMEC. Metabolites were ranked based on \log_2 fold change of senescent/proliferating. Shown are the mountain plot of nucleoside mono/di/tri-phosphates (left), and table of all tested metabolic pathways (right).



Supporting Fig. S2: [U-¹³C]-labeled glucose isotopomer distributions are not altered in senescent HMEC.

A-B) [U-¹³C]-labeled glucose isotopomer distributions of citrate and fumarate. Proliferating and senescent HMEC show similar labeling patterns for TCA cycle metabolites. See Supporting Table S3 for all measured metabolite isotopomer distributions.



Supporting Fig. S3: [1,2-¹³C]-glucose and [U-¹³C]-glutamine stable isotope tracing

A) [1,2-¹³C]-labeled glucose isotopomer distribution. The ratio of M1 to M2 lactate does not show a significant change between proliferating and senescent HMEC.

B) Fractional contribution of [1,2-¹³C]-glucose to purines and pyrimidines is downregulated in senescent HMEC. Volcano plot represents \log_2 fold change (senescent/proliferating) for fractional contribution of [1,2-¹³C]-glucose and FDR-corrected p-value.

C) Metabolic pathway map depicting the average \log_2 fold change (senescent/proliferating) of fractional contribution of [1,2-¹³C]-glucose using the indicated color scale. Metabolites that were not measured are shown as small grey colored shapes.

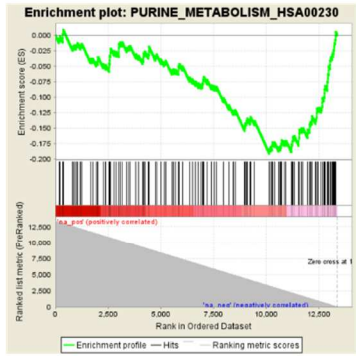
D) [U-¹³C]-labeled glutamine isotopomer distributions for TCA cycle metabolites. The ratio of reductive to oxidative TCA cycle is slightly decreased in senescent HMEC.

E) Fractional contribution of [U-¹³C]-glutamine to pyrimidines is downregulated in senescent HMEC. Volcano plot represents average \log_2 fold change (senescent/proliferating) for fractional contribution of [U-¹³C]-labeled glutamine and FDR-corrected combined Fisher's combined p-value from two independent experiments.

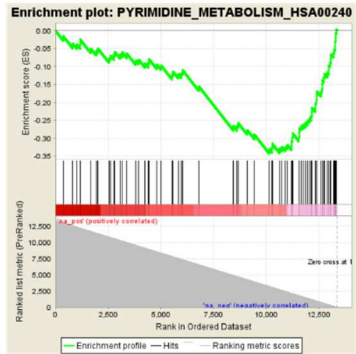
F) Metabolic pathway map depicting the average \log_2 fold change (senescent/proliferating) of fractional contribution of [U-¹³C]-glutamine using the indicated color scale. Metabolites that were not measured or had less than 3% fractional contribution are shown as small grey colored shapes.

A)

HMEC



Normalized enrichment score	-2.59
Nominal p-value	< 0.001
FDR q-value	0.001

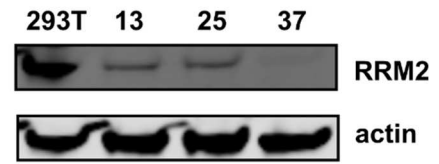


Normalized enrichment score	-3.51
Nominal p-value	< 0.001
FDR q-value	< 0.001

Higher abundance in senescent HMEC Higher abundance in proliferating HMEC

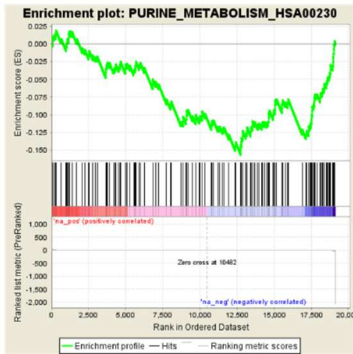
C)

HMEC PD

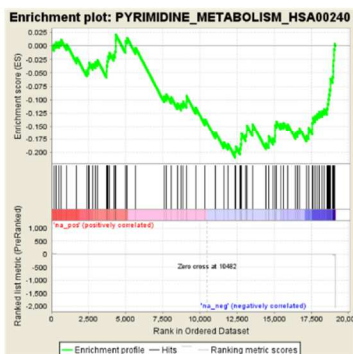


B)

IMR90



Normalized enrichment score	-2.22
Nominal p-value	0.0012
FDR q-value	0.016



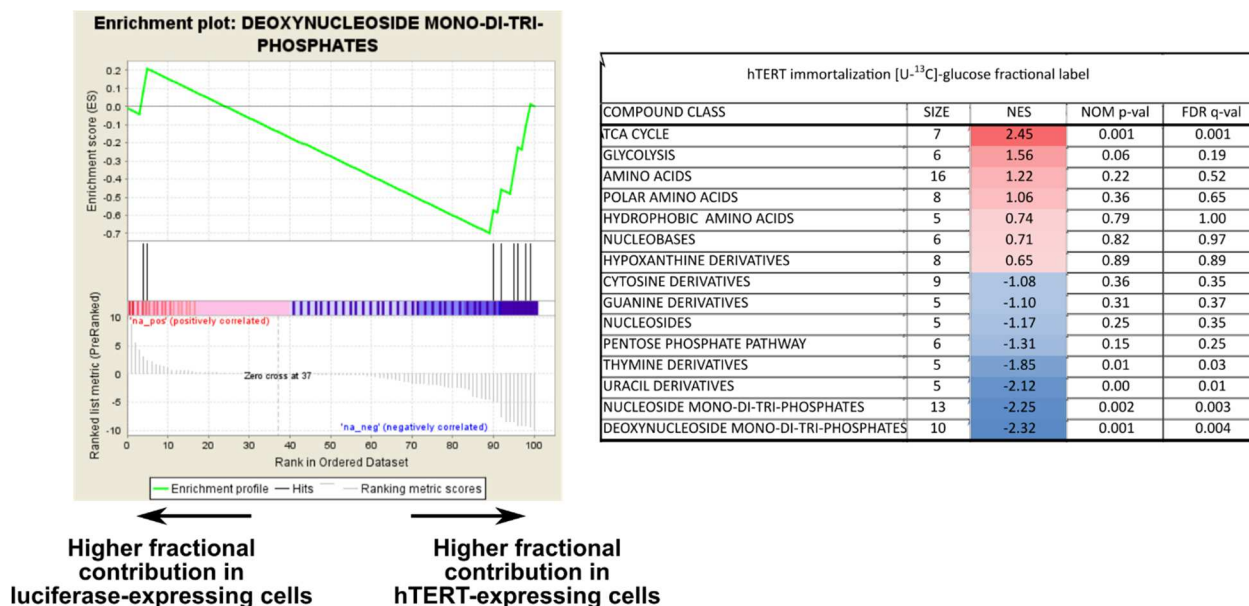
Normalized enrichment score	-2.29
Nominal p-value	0.0004
FDR q-value	0.015

Higher abundance in control IMR90 Higher abundance in senescent IMR90

Supporting Fig. S4: RNA expression analysis confirms reduced nucleotide synthesis in senescent cells.

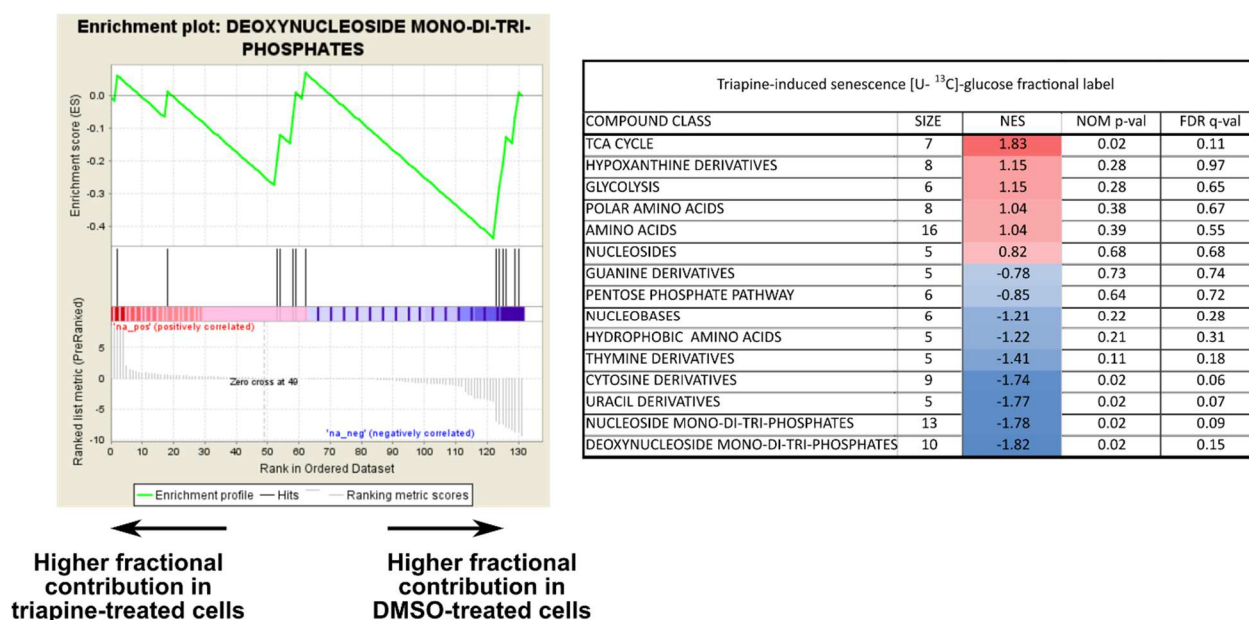
A-B) GSEA analysis of A) microarray data from senescent HMEC (1) and B) RNAseq data from senescent IMR90 cells (2). For HMEC microarray data, genes were compared across pairwise comparisons for stasis and pre-stasis cell cultures. Genes were then ranked by their average rank from individual experiments. For IMR90 RNAseq data, genes were ranked based on signal to noise ratio of senescent/non-senescent. Results show significant suppression of genes in the purine (hsa00230) and pyrimidine (hsa00240) pathways in senescent cells.

C) Western blotting with an RRM2 antibody (Sigma) targeting a distinct epitope from Figure 3E revealed downregulation of RRM2 expression in senescent HMEC. Actin was used as an equal loading control.



Supporting Fig. S5: Metabolite set enrichment analysis of hTERT immortalization.

MSEA analysis for fractional contribution of [U-¹³C]-glucose in hTERT immortalized HMEC. Metabolites were ranked based on log₂ fold change of luciferase/hTERT.



Supporting Fig. S6: Metabolite set enrichment analysis of triapine-induced senescence.

MSEA analysis for fractional contribution of [U-¹³C]-glucose in triapine-induced senescence. Metabolites were ranked based on log₂ of triapine/DMSO.

REFERENCES

1. Garbe, J. C., Bhattacharya, S., Merchant, B., Bassett, E., Swisshelm, K., Feiler, H. S., Wyrobek, A. J., and Stampfer, M. R. (2009) Molecular Distinctions between Stasis and Telomere Attrition Senescence Barriers Shown by Long-term Culture of Normal Human Mammary Epithelial Cells. *Cancer Res.* **69**, 7557–7568
2. Baar, M. P., Brandt, R. M. C., Putavet, D. A., Klein, J. D. D., Derks, K. W. J., Bourgeois, B. R. M., Stryeck, S., Rijksen, Y., van Willigenburg, H., Feijtel, D. A., van der Pluijm, I., Essers, J., van Cappellen, W. A., van IJcken, W. F., Houtsmuller, A. B., Pothof, J., de Bruin, R. W. F., Madl, T., Hoeijmakers, J. H. J., Campisi, J., and de Keizer, P. L. J. (2017) Targeted Apoptosis of Senescent Cells Restores Tissue Homeostasis in Response to Chemotoxicity and Aging. *Cell.* **169**, 132-147.e16